
Fault Injection for Electrical System in More Electric Aircraft

Zhiyong Fan^{1,*}, Zhen Zhao², Yigang Sun³, Zhexu Liu²

¹Engineering technology training center

²College of electronic information & automation

³College of Aerospace Automation, Civil Aviation University of China, Tianjin, 300300, China

*Corresponding Author: Zhiyong Fan

Abstract:

Electrical system plays an important role in the running state and operation safety of more electric aircraft. In this paper, we consider the modelling problem of the electrical system in more electric aircraft. To this purpose, a normal model of the system is built in AMESim based on detailed analysis of the mechanism of the system. Furthermore, fault injection function is extended on the basis of the normal model, to realize not only normal simulation, but also fault simulation of the system. Extensive simulation results are given to illustrate the feasibility and effectiveness of the established model.

Keywords: More electric aircraft, fault injection model, co-simulation, AMESim

I. INTRODUCTION

By employing electric energy to replace traditional hydraulic and pneumatic energy system, More electric aircraft (Abbreviated as MEA) can greatly simplify internal architecture of the aircraft [1], increase reliability [2,3], efficiency, survivability, and reduces weight, fuel consumption, and cost [4]. Due to the characteristic and superiority, MEA has been the development tendency of modern aircraft, and has attracted a large quantity of attention by researchers and institutes [5].

However, the anticipated development of MEA leads to diversified power-supply demands, which brings new difficulties and challenges to diagnose fault, isolate fault, predict fault, allocate power, and manage load for the electrical system in MEA. Fault injection for electrical system in MEA is a process to carry out fault mode analysis, fault modeling, and fault injection experiment in the system, whose result can be used to validate whether the control unit in the presence of fault can be effective for processing, to trigger potential faults and design flaws in the system, so as to find out the countermeasures, correct system design, and shorten the design cycle. According to the result analysis after fault injection, the reliability of the system is tested.

Fault injection technology has been applied in some fields, such as circuit [6], flight control [7], etc., and have obtained satisfactory experimental results. A Purvis [7], et al., took A380 as the research object, modeled the key control system, copied the established functional model into the hardware and software system to inject faults into the system, and detected these faults. Nikos Foutris [8], et al., presented a general architecture level fault injection framework, which took a microprocessor as the research object, carried on the fast effective injection to the processor hardware different fault mode, analyzed the result, and verified the processor hardware reliability. Erik van der Kouwe [9], et al., presented a method to evaluate whether the injected fault matches the set fault model and analyzes which factors cause the deviation between the injected fault and the set fault model. Wang Chao [10], et al., proposed a fault injection tool based on simulation to study the fault propagation in application and the fault performance at the system level, especially the fault performance of the deep cause. Aguirre M.A. [11], et al., presented a fault injection method for bidirectional signal, which solved the reliability problem of bidirectional port. Chang Qing [12], et al., proposed a fault injection method based on in-machine testing. Prodan Lucian [13], et al., presented a fault injection method for quantum circuit, which compared the fault injection circuit with the correct circuit, determined the fault rate and cause of the fault injection circuit, and determined the influence of the fault on the circuit. In short, fault injection is generally mature in software testing, network and circuit, but there is less research on the fault transfer mode of the electrical system of more electrical aircraft. The application of and there are few references on the fault injection of the electric aircraft.

To diagnose fault, test, and carry on safety analysis for the electrical system in MEA, it is necessary to build feasible simulation model for the system, which can both simulate normal operation, and also simulate faulty operation. This paper is taking the electrical system of the MEA as the research object to study the fault injection method in the system for further analysis.

The rest of this paper is organized as follows. The mechanism of a typical electrical system of a MEA is introduced in Section 2. In Section 3, the typical electrical system is modeled to simulate normal operation of the system. Based on the normal model, fault injection function is added to realize fault simulation. Based on the electrical system model of the MEA, the feasibility and effectiveness is verified in a co-simulation platform in Section 4. The conclusion of this paper is drawn in Section 5.

II. MECHANISM OF ELECTRICAL SYSTEM IN MEA

2.1 Electrical System

Fig. 1 illustrates a typical electrical system in a MEA, which is consisted with the power system, distribution network, and electrical equipment. The main power supply of the aircraft is composed of four frequency conversion starting generators (VFSG), i.e., VFSG L1, VFSG L2, VFSG R1, and VFSG R2, each of which is connected to the corresponding 235V main ac bus bar, i.e., 230VAC_L1, 230VAC_L2, 230VAC_R1, and 230VAC_R2. The auxiliary power

supply consists of two auxiliary variable frequency starting generators (ASG), i.e., ASG L and ASG R in Fig. 1, each of which is connected to the corresponding 235V auxiliary ac bus bar, i.e., LTB and RTB. The emergency power supply consists of emergency generators (rats), RAT in Fig. 1, which are connected to a backup bus bar, Bkup bus. In addition, there is a main battery and an APU battery on board, which are connected to the pilot instrument bus bar and the co-pilot instrument bus bar, respectively.

The load on the aircraft is divided into dc load and ac load. Dc load is divided into high-voltage dc load and low-voltage dc load. Ac load is divided into high-voltage ac load and low-voltage ac load. When powering these loads, the electric energy of the aircraft needs to provide different voltage values according to the demands of the loads.

The distribution network consists of transformer (L_ATU and R_ATU in Fig. 1), variable voltage rectifier (L_TRU and R_TRU in Fig. 1), auto-transformer rectifier (ATRU L1, ATRU L2, ATRU R1, and ATRU R2 in Fig. 1), BUS, contactor, circuit breaker, switch, and other necessary components. ATU is to convert 235VAC into 115VAC, connect to 115VAC bus bar, and supply power to electric load of 115VAC. TRU is to convert 235VAC voltage into 28VDC, and connect it to the bus bar of 28VDC, the bus bar of captain instrument, and the bus bar of co-pilot instrument, to supply power for the load of 28VDC. ATRU converts 235VAC into 270VDC, which supplies power for the high-voltage dc load on the aircraft.

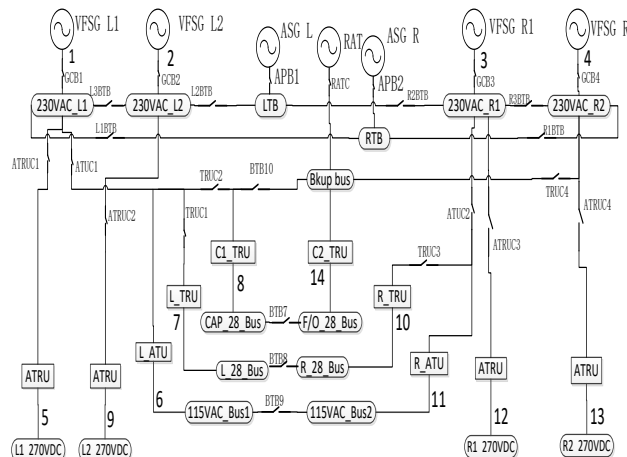


Fig 1: diagram of a typical electrical system of a MEA

Under normal working conditions, the four starting generators VFSG work, while ASG and RAT do not work. The power supplied by the four generator is connected to four 235VAC main bus bars. The contactors between the main bus bars are disconnected. The power transmitted by the four main bus bars is connected to the power conversion devices and a portion of the high-power loads. The entire power network is in four separate power supply lines. If a component on any one of the lines occurs a fault, the corresponding controller will disconnect the control switch and isolate the fault from the power supply network. Meanwhile, the bus bar that loses power will get power from the bus bar with the same grade, ensuring the power supply for the load on it.

If all AC power supply fails during the flight, the backup electrical system (backup bus bar) will automatically provide 28VDC power to the pilot instrument bus bar, co-pilot instrument bus bar, communication equipment, and navigation equipment. Under this situation, an independent flight control dc electrical system provides enough energy for the telex flight control system to ensure flight safety. If all engines fail, RATs provide hydraulic power to the central hydraulic system, and supply power to the backup bus bars of aircraft. By controlling the on and off of the power and switches, the loads can be selected from different bus bars, and the combination of these loads replaces the ground service and the flight backup system.

2.2 Fault Mode in the Electrical System

According to the components in the electrical system, we can derive the fault for each type of components in the following context.

(1) Fault of starter/generator

The starter/generators in a typical MEA (B787) are three-phase brushless frequency conversion alternators [14], whose schematic diagram is as shown in Fig. 2.

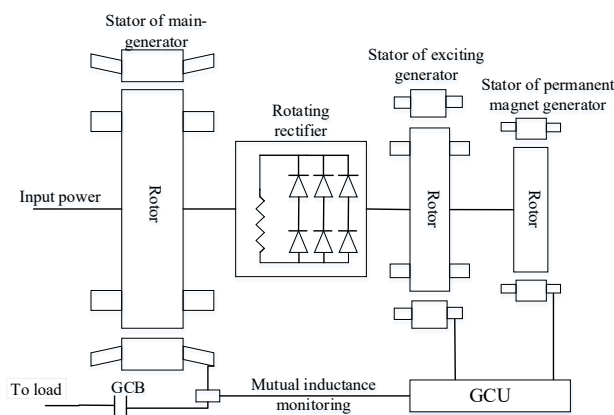


Fig 2: schematic diagram of generators in B787

The output voltage of the generator is related to the voltage provided by GCU to the stator of the exciter. When the voltage provided by GCU to the stator of the exciter is too high or too small, that is, the regulator fails, the output voltage of the generator will produce overvoltage or under-voltage phenomenon. The insulation performance of stator and rotor coil on the generator is a key factor affecting the quality of the generator' output voltage, and the degraded insulation performance may cause the over-voltage and under-voltage fault. When the speed generator occurs a problem, the output voltage frequency of the generator is over-frequency or under-frequency. When internal output winding is open circuited, or the external feeder is open circuited, or the output contactor has a bad contact or damage, the generator' output would occur an open phase fault. In conclusion, the fault modes of the generator are voltage overvoltage, voltage under-voltage, voltage over-frequency, voltage under-frequency, output voltage fluctuation, and no output.

(2) Fault of Transformer

The operation process of transformer is always affected by thermal, electrical, mechanical stress, and environmental factors for a long time, which may cause insulation aging, iron core and winding failure, resulting in output deviation from the normal value, and finally leading voltage overvoltage, voltage under-voltage fault, short circuit fault, open circuit fault, and overheating fault.

(3) Fault of transformer-rectifier (TR)

The principle of transformer-rectifier can be divided into two parts: variable-voltage and rectifier, as shown in Fig. 3. The principle of variable-voltage part is the same as that of transformer, so there are overvoltage and under-voltage fault for the transformer-rectifier.

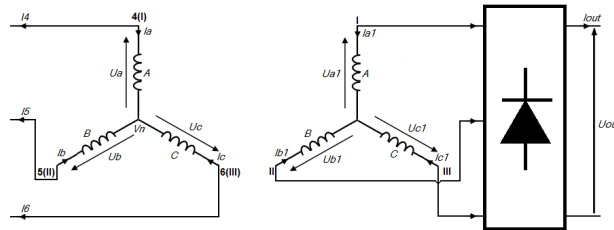


Fig 3: principle of TR

The variables in TR satisfies the following relationship.

$$I_{out} = -I_2 \quad (1)$$

$$U_{out} = \frac{U_{dcnom} \cdot U_{rms}}{U_{acnom}} \quad (2)$$

where, I_{out} is the output current of TR, U_{out} is the output voltage of TR, U_{rms} is the Valid value of input voltage, U_{dcnom} and U_{acnom} are the DC Amount and alternating current component of the input voltage.

(4) Fault of bus bar

The bus bar is divided into ac bus bar and dc bus bar, which are structurally identical. The input of the bus bar is generally composed of one terminal, and the output end connects to different load. By changing the number of ports at both ends of the bus bar, the number of loads connected to the bus bar can be changed. The connection between each load and the bus bar can be equivalent to one terminal, so the output of the bus bar can be equivalent to the collection of different numbers of terminals. When the input feeder or output feeder of the bus bar is broken, the bus bar will lose power, and the open circuit fault will occur. The carrying capacity of the bus bar is related to the allowable temperature rise. When the temperature of the bus bar exceeds a certain limit value, the bus bar will occur overheat fault. Due to the influence of the external environment, for example, vibration during the flight of the aircraft, the insulation layer will be damaged, which makes the conductive layer of the bus bar come into contact with each other, and cause short-circuit fault. In conclusion, there are open-circuit fault, short-circuit fault, and overheat fault for the bus bar.

(5) Fault of switch

There are lots of relays, contactors, switches, and other switch components in multi-electric systems, through which, the control of aircraft load power supply can be realized. Switch fault is divided into two types, one is when the instruction indicates that the switch is disconnected, the switch cannot be disconnected; the other is when the instruction tells the switch to close, the switch cannot close.

III. MODELLING OF ELECTRICAL SYSTEM IN MEA

Base on the mechanism of the electrical system in MEA, the normal model is established in this section based on AMESim (Advanced Modeling Environment for Simulation of engineering systems) software, which is launched by the French Imagine company in 1995, and has been widely used in modeling, simulation, and dynamics analysis for hydraulic/mechanical/electrical system. To serve for further fault diagnosis, test, and safety analysis, the fault injection model is built based on the normal model of the electrical system in MEA.

3.1 Normal Model

AMESim is the hydraulic/mechanical system modeling, simulation and dynamics analysis software based on power bond diagram introduced by French Imagine company in 1995 [15]. In AMESim, there are some basic model components for the electrical system of aircraft, such as generator module, autotransformer rectifier module, transformer module, bus bar module, contactor module, general load module, and so on, which can be dragged from the module library to build the desired model. Then, these selected modules can be connected according to the mechanism analyzed in Section 2 to compose the whole electrical system of MEA.

In the modeling process using AMESim, the setting of parameters has a great impact on the accuracy of the system model, so the difficulty of modeling lies in the setting of model parameters and the matching of the whole model elements. In this paper, firstly, the parameters of a component are set to match the actual electrical system components as much as possible, and the components are tested. The components that pass the test are taken as part of the whole model, and then the next component is tested. The components that pass the test are put together with the original components to form an electrical channel model. The same method is used to build the rest of the electrical channel model, and finally connect the electrical channels together to form the whole model of the entire electrical network. The whole model of the electrical system in MEA under normal state is as shown in Fig. 4.

The generators used in the normal model is three-phase variable frequency generators with RMS voltage input port and frequency input port. In AMESim, the three-phase output voltage of the generator can be controlled by setting the input voltage of the generator, and the output voltage of generator can be selected as valid value or sine wave during simulation process. In practical system, the valid value of the three phase voltage is 235V, and the peak voltage is 332V.

In the model shown in Fig. 4, the generator connects to the switch and to the bus bar. If the switch is closed, the three-phase AC can outputs to the bus bar. While in AMESim, there are

three output ports for the generator, which cannot directly connect to the one input port of the bus bar. Therefore, a converter element is required to convert three terminals to one terminal. In this way, the bus bar uses a terminal to distribute power in the model, which represents a three-phase alternating current instead of a one-phase alternating current. The bus bar is then connected to the ATRU. Due to different number of terminals of the two components, a converter element is also required to convert one terminal to three terminals between the two components. In practical system, the output voltage of the ATRU is $\pm 270\text{V}$, and the voltage difference between the two ends of the ATRU is 540V . In the simulation model, an equivalent method is adopted to ground at one end and set the voltage at the other end as 540V . In practical system, the effective value of the output voltage of the ATU is 115V . While in the simulation model, the transformer ratio is set appropriately to obtain the regular voltage and frequency under normal operation state.

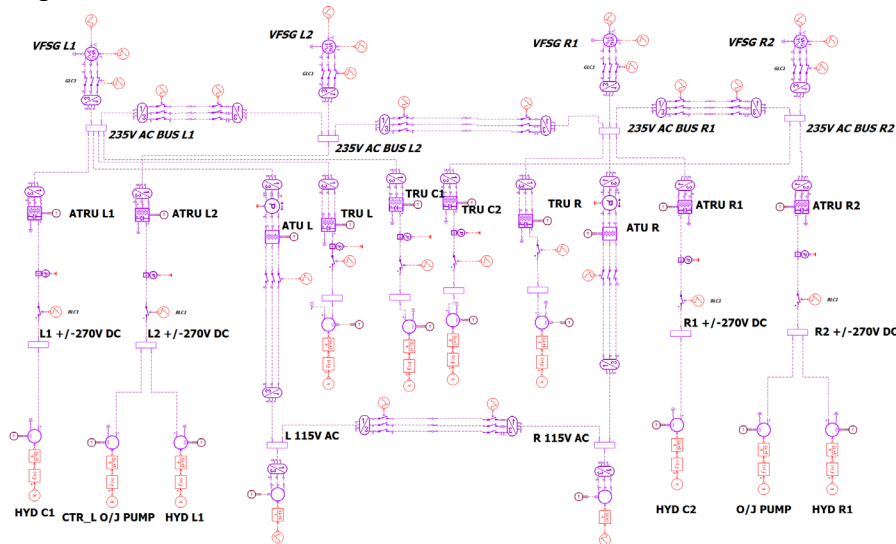


Fig 4: normal model of the electrical system in MEA

In the normal model, the power detection element is added to detect the power value in the current line to prevent overload fault. The bus bar is connected with ac load and dc load, whose power value can be changed to simulate load increase or unloading.

The parameters in the normal model is selected according to the U.S. military standard MIL-STD-704F, which stipulates the electric energy index of aircraft in steady state operation, shown in TABLE I and II.

According to TABLE I and II, the effective value of the input voltage of the four generators are all set as 230V , and the frequency of the voltage are set as $380\sim 800\text{Hz}$. To simulate the actual frequency conversion characteristics of the generators, the switches between the generators and 230V bus bar, ATU and 115V bus bar, ATRU and 270V bus bar, TRU and 28V bus bar are all closed, the switches between 230V bus bar and 115V bus bar are disconnected, and the operation of the electrical system in MEA is tested. Figs. 5-7 illustrate the operation results.

TABLE I. Electric energy index of aircraft in steady state operation for AC

Index	AC 230V	AC 115V
Phase voltage/V	208.0~244.0	108.0~118.0
Frequency/Hz	360~800	360~800

Table II. Electric energy index of aircraft in steady state operation for DC

Index	DC 270V	DC 28V
Voltage/V	250.0~280.0	22.0~29.0

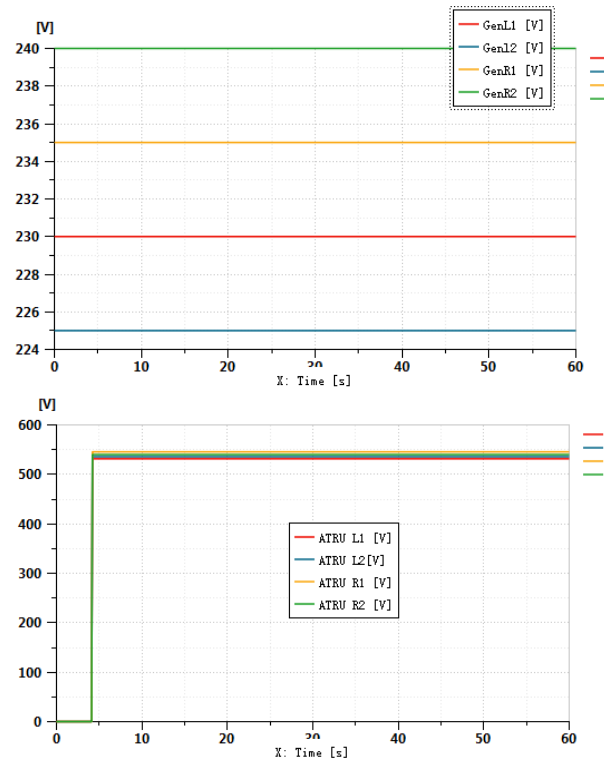
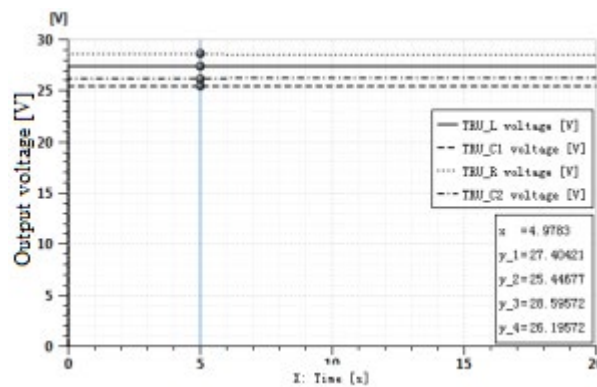


Fig 5: output voltage of the generators and the ATRU



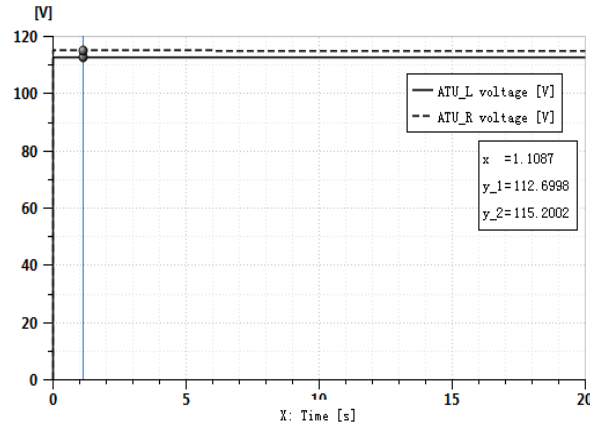


Fig 6: output voltage of TRU and ATU

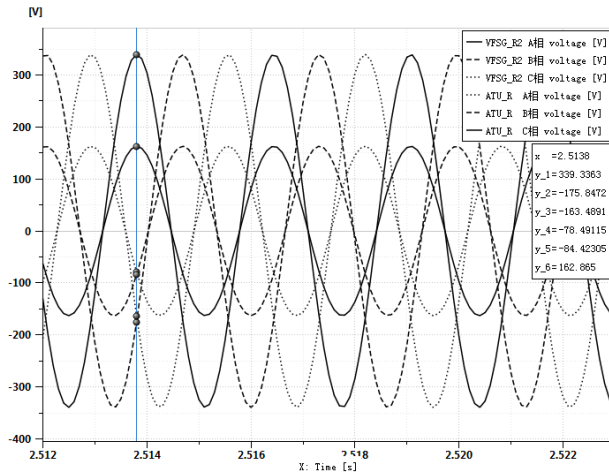


Fig 7: output sine voltage of the generators and the ATRU

From Fig. 5 and 6, it can be seen that the effective value of the generators is among 215V~240V, the output voltage of ATRU is among 255V~276V, and the output voltage of TRU is among 25V~28.6V. The results are consistent with the electric energy indices stipulated in TABLE I and II. From Fig. 7, the frequency of output voltage of the generators is 400Hz, which is also satisfied regulations stipulated in TABLE I.

In conclusion, the established model in Fig. 4 can realize simulation of the electrical system in MEA under normal operation.

3.2 Fault Injection Model

According to the fault modes in the electrical system in MEA analyzed in Section 2.2, the fault injection model is to improve the normal model by adding fault injection function. The fault injection function is expanded for the main component in the electrical system in MEA.

(1) Fault injection sub-model for the generator

The RMS voltage input port and frequency input port are selected as the data interaction interface of the simulation element.

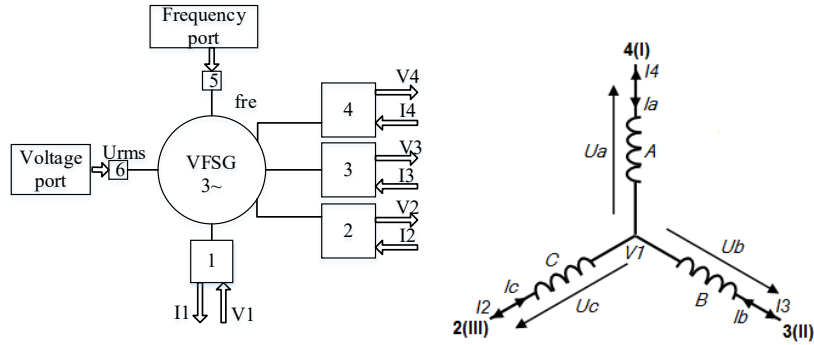


Fig 8: diagram of fault injection sub-model for the generator

In Fig. 8, V_1 is the neutral voltage of the AMESim model of the generator; V_2 , V_3 , and V_4 are the output phase voltages of the AMESim model of the generator, respectively; U_{rms} and f_{re} is the effective value and frequency of voltage of the AMESim model of the generator; I_1 , I_2 , I_3 , and I_4 are the corresponding feedback current of the related ports; U_a , U_b , and U_c represents the three-phase voltage respectively.

The voltage of the generator is as Eq. (3).

$$\begin{aligned} U_a &= U_{rms} \cdot \sqrt{2} \cdot \sin(2\pi \cdot wt) \\ U_b &= U_{rms} \cdot \sqrt{2} \cdot \sin\left(2\pi \cdot wt - \frac{2\pi}{3}\right) \\ U_c &= U_{rms} \cdot \sqrt{2} \cdot \sin\left(2\pi \cdot wt + \frac{2\pi}{3}\right) \end{aligned} \quad (3)$$

The output voltage of the AMESim model of the generator is as Eq. (4).

$$\begin{aligned} V_2 &= V_1 + U_c \\ V_3 &= V_1 + U_b \\ V_4 &= V_1 + U_a \end{aligned} \quad (4)$$

The fault injection function in the sub-model of the generator is realized by selecting the voltage port '6' and frequency port '5' as data interaction interfaces with external model, to set overvoltage fault, undervoltage fault, overfrequency fault, underfrequency fault, output voltage fluctuation fault. The feedback current I_1 numerically equals to the algebraic sum of three-phase feedback currents I_2 , I_3 , and I_4 , which can be used to determine whether the generator is overloaded.

(2) Fault injection sub-model for the transformer

Fig. 8 illustrates the schematic diagram of ATU, in which V_n is neutral potential of the primary coil; U_a , U_b , and U_c are the phase voltages of the primary coil; I_5 , I_6 , and I_7 are the feedback currents of the primary coil; I_1 , I_2 , and I_3 are the feedback currents of the secondary coil. Fig. 10 gives the encapsulation model and fault injection sub-model of ATU.

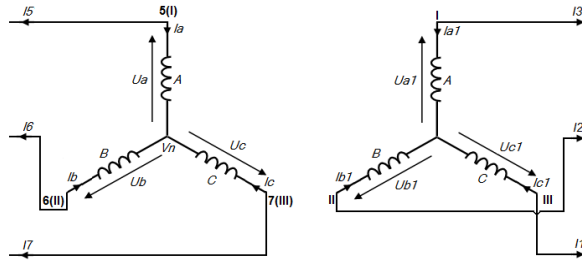


Fig 9: schematic diagram of ATU

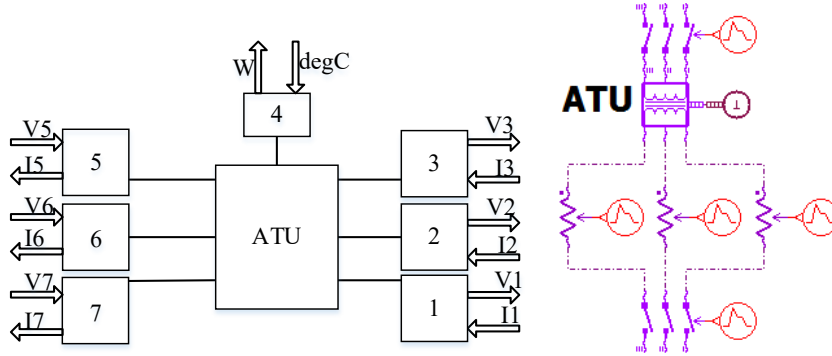


Fig 10: encapsulation model and fault injection sub-model of ATU

The relationship among parameters in ATU is as below:

$$V_n = \frac{V_5 + V_6 + V_7}{3} \quad (3)$$

$$U_a = V_5 - V_n$$

$$U_b = V_6 - V_n$$

$$U_c = V_7 - V_n$$

$$U_{rmsin} = \frac{\sqrt{U_a^2 + U_b^2 + U_c^2}}{3}$$

$$U_{rmsout} = ratio \cdot U_{rmsin} \quad (5)$$

$$I_{rmsout} = \frac{\sqrt{I_1^2 + I_2^2 + I_3^2}}{3}$$

where, U_{rmsin} and U_{rmsout} are the effective value of the input voltage and the output voltage, respectively; I_{rmsout} is the effective value of the output current; *ratio* is transformation ratio.

For the open circuit fault, there may be three possibilities, open circuit of the input line, open circuit of the output line, and transformer breaker. For the first possibility, fault injection can be realized by adding a switch in the input line to simulate the running state of the input line. For the latter two possibilities, the input voltage is normal, while the output voltage is 0. Therefore, the fault injection can be realized by setting a switch in the output line, which can be controlled through external ports. For the overvoltage fault and under-voltage fault, the fault injection can be realized by cascading a variable resistance in the output line. If the variable resistance is small, then overvoltage fault occurs, vice versa.

(3) Fault injection sub-model for the transformer-rectifier (TR)

The package diagram of TR in AMESim and the fault injection sub-model is illustrated in Fig. 11. The external variables of TR are three input voltage interfaces, whose input is voltage and feedback is current, one input set interface, whose set quantity is temperature and feedback quantity is heat, and two output voltage interfaces, one of which with voltage output and current feedback, another with current output and voltage feedback. In the fault injection sub-model, a slide rheostat is applied in the output interface of TR to simulate over-voltage or under-voltage fault; two switches are introduced in the input and output interface of TR to change the input and output states of TR by adjusting control signal for each switch.

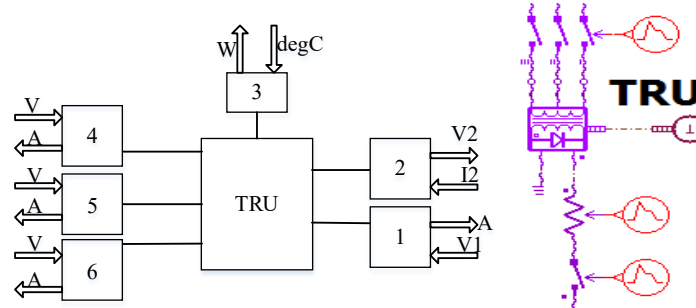


Figure 11: package diagram of TR and the fault injection sub-model

(3) Fault injection sub-model for the Bus Bar

When establishing fault injection sub-model for the bus bar, controllable switches are added in the input lines and the output lines. By controlling the on and off of these controllable switches, the open-circuit fault and short-circuit fault can be simulated for each line of the bus bar.

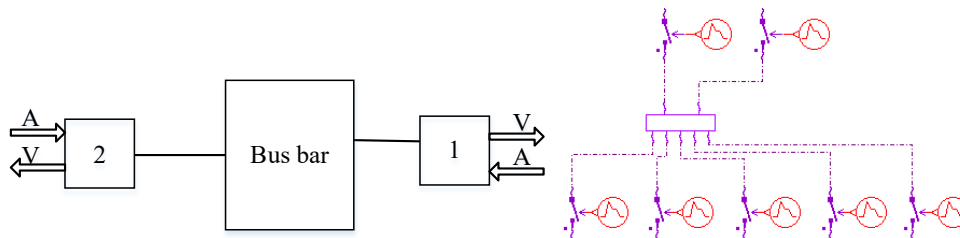


Figure 12: package diagram and the fault injection sub-model of the bus bar

IV. CO-SIMULATION VERIFICATION

Aircraft co-simulation is the process of integrating models of different fields established by different simulation software (including AMESim model of aircraft electrical system and hydraulic model, control model established by Matlab, flight dynamics model built with FlightSim, etc) into simulation verification. Compared to single model verification, the co-simulation can provide more information in verifying the affection of the electrical system on the other system in the aircraft.

4.1 Co-Simulation Platform

Fig. 13 illustrates the principle of the co-simulation platform of MEA, in which, each interface library of simulation software or language co-simulation model (including Matlab/Simulink, Matlab M file, AMESim, Saber, Labview, FlightSIM, Rhapsody, C/C++,

etc.), simulation software, or program language, achieve distributed co-simulation through the interface. During the fault injection process, the injected fault in the electrical system would also transmit to the other aircraft system through the DDS soft bus, for that the electrical system model of the MEA built in AMESim is connected to the DDS soft bus.

Fig. 14 is the practical co-simulation platform established in our lab, which contain 12 computers operating different sub-models.

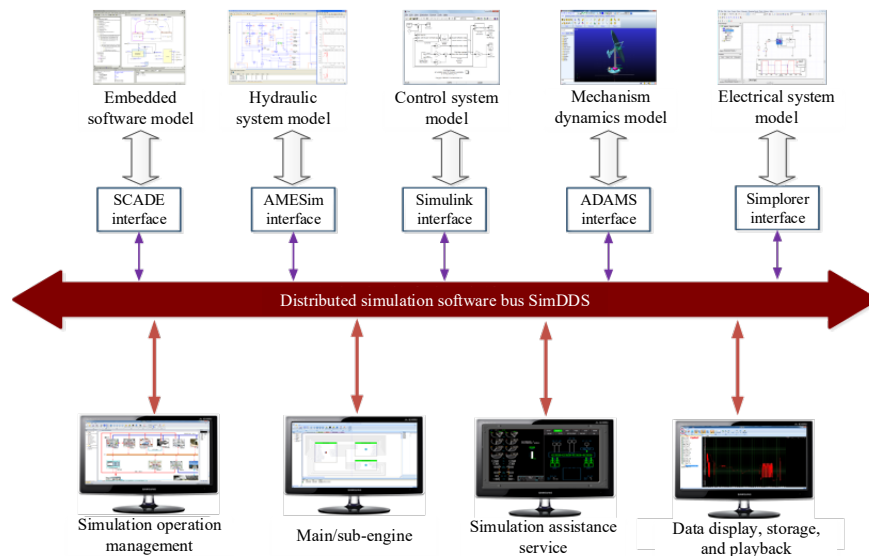


Fig 13: structure of co-simulation platform

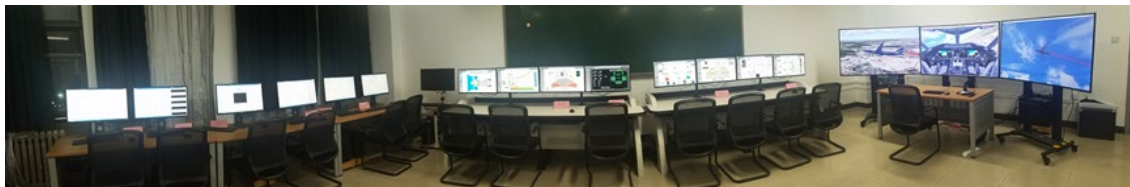


Fig 14: co-simulation platform of MEA

4.2 Result and Discussion

(1) Simulation of fault in the generator

Owing to spatial confined, this paper selects three types of faults in the generator, i.e. overvoltage fault of Generator L1, under-voltage fault of Generator L1 and L2, and overvoltage fault of Generator R1. For the first type of fault, the set fault is the change process of the output voltage of the generator from the normal value of 235V to 285V and then back to 235V. For the second type of fault, the under-voltage fault of L1 is set as the change process of the output voltage of L1 from the normal value 235V to 205V and then back to 235V, the under-voltage fault of L2 is set as the change process of the output voltage of L2 from the normal value 235V to 205V and then back to 235V. For the third type of fault, the fault is set as that the output voltage of R1 decreases from the normal value to 205V, which is cut off after 7s, and the power is supplied by the generator R2.

Figs. 15-16 show the voltage value in the electrical system and the load. From these two figures, it can be seen that, when the output voltage of L1 changes from 235V to 260V, the output value of TR C1 changes from 28V to 32V, and the voltage of transformer changes from 115V to 127.4V, and the output voltage of ATRU changes from 270V to 298.8V. The voltage of load connected to the bus bar is consistent with that of the power conversion device. The load voltage on the 270V bus bar is 298.2V, and the effective voltage value of the load on the 115V ac bus bar is 127.4V, and the effective voltage value of the load on the 235V ac bus bar is 259.99V, and the load voltage on the left 28V DC bus bar is 30.9V, in the case of overvoltage. It can be concluded that the overvoltage fault of L1 is transmitted to the 235V ac bus bar, causing overvoltage at both ends of the load connected to the bus bar, and further causing the output overvoltage of TR and automatic transformer respectively, and finally the overvoltage fault is transmitted to the bus bar connected to power conversion elements, and leading overvoltage of the loads connected to the bus bar.

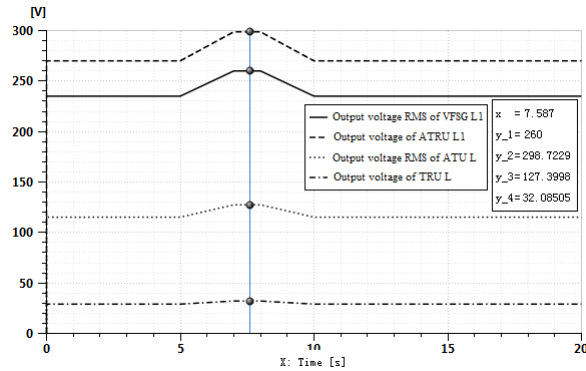


Fig 15: output voltage of VFSG L1, ATRU L1, ATU L, TRU L for overvoltage fault of VFSG L1

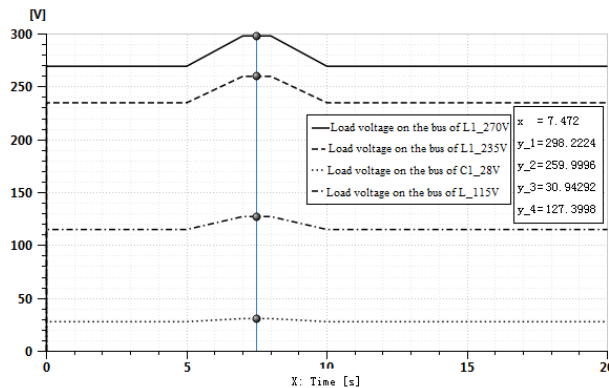


Fig 16: load voltage for overvoltage fault of VFSG L1

Figs. 17-18 illustrate the results for the under-voltage fault of VFSG L1 and L2. From these two figures, it can be seen that the voltage of VFSG L1 drops, maintains and returns to normal during 1s~8s, and the voltage of VFSG L2 drops, maintains and returns to normal during 5s~13s. In this process, the voltage of VFSG L1 decreases from 235V to 205V during 1s~5s, and the voltage of TR L decreases from 29V to 25V, that of transformer decreases from 115V

to 100V, and that of ATRU from 267V to 235V. During 0s~5s, the voltage of VFSG L2 remains unchanged. During 5s~10s, the voltage of VFSG L2 decreases from 235V to 185V, and the output voltage of ATRU changes from 267V to 212V. The voltage of VFSG L1 returns to the normal 235V level at 8s, while the voltage of VFSG L2 returns to the normal 235V level at 13s. The voltage of other power conversion elements and loads changes in line with the voltage of VFSG L1/L2.

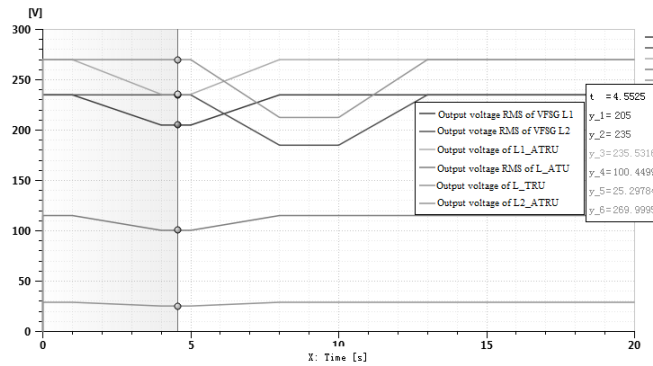


Fig 17: voltage when occurring undervoltage fault of VFSG L1/L2

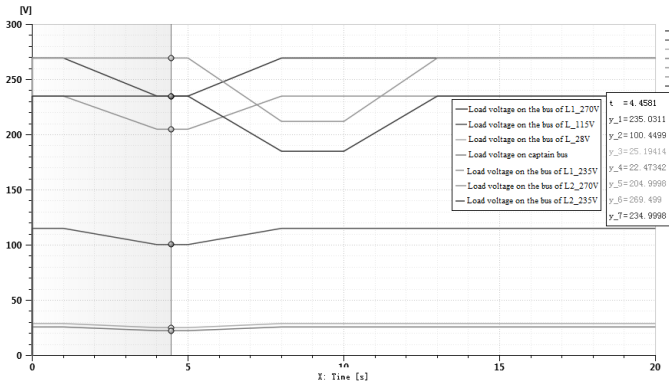


Fig 18: Load voltage when occurring undervoltage fault of VFSG L1/L2

Figs. 19-20 give the output voltage of VFSG R1, R2, and the connected power conversion elements. It can be seen that the output voltage of VFSG R1 is in the normal range during the whole process, while VFSG R2 turns off at 5s, and the output voltage of C2_TRU and R2_ATRU supplied by VFSG R2 is 0V, and the switch between the bus bar R1_235V and R2_235V is closed, and the bus bar R2_235V is powered by R1_235V, and the output of R2_ATRU and C2_TRU return to normal. This shows that when the power of the bus bar is lost due to the fault of the generator, other alternative bus bars can be supplied to ensure the power reliability of the load, which verifies the feasibility of this fault scheme.

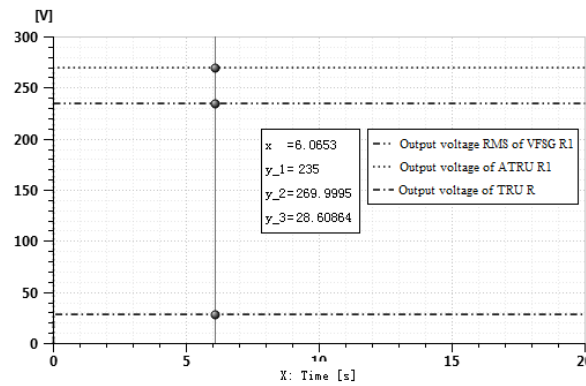


Fig 19: voltage of VFSG R1, ATRU R1 and TRU R

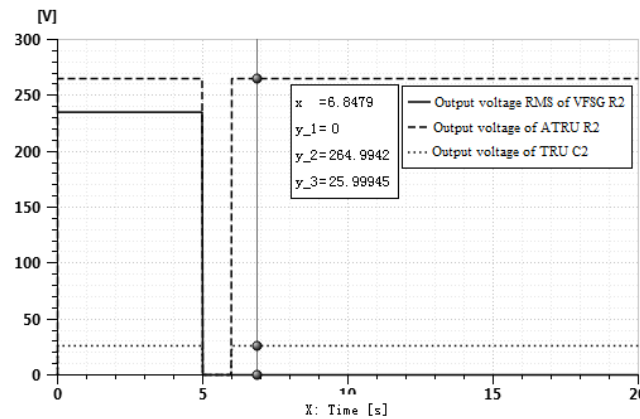


Fig 20: voltage of VFSG R2, ATRU R2 and TRU C2

(2) Simulation of fault in transformer

Figs. 21-22 give the overvoltage fault and under-voltage fault of ATU. From Fig. 21, the output voltage of ATU L increases from 115V to 123V, when its input voltage is under normal 235V, which occurs overvoltage fault. While for Fig. 22, it occurs under-voltage fault for ATU L.

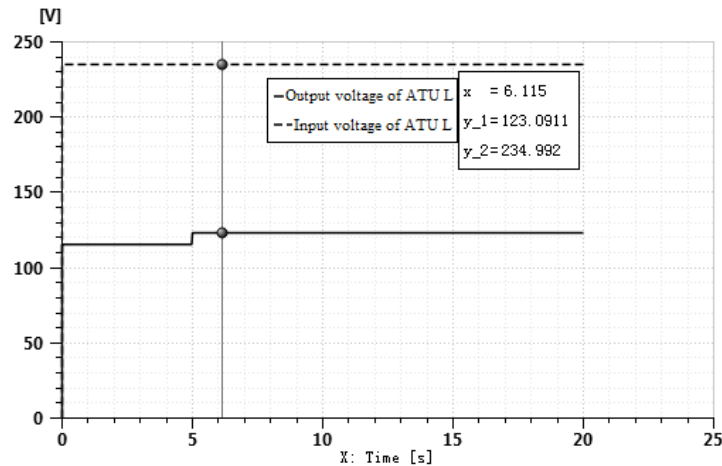


Fig 21: overvoltage fault of ATU L

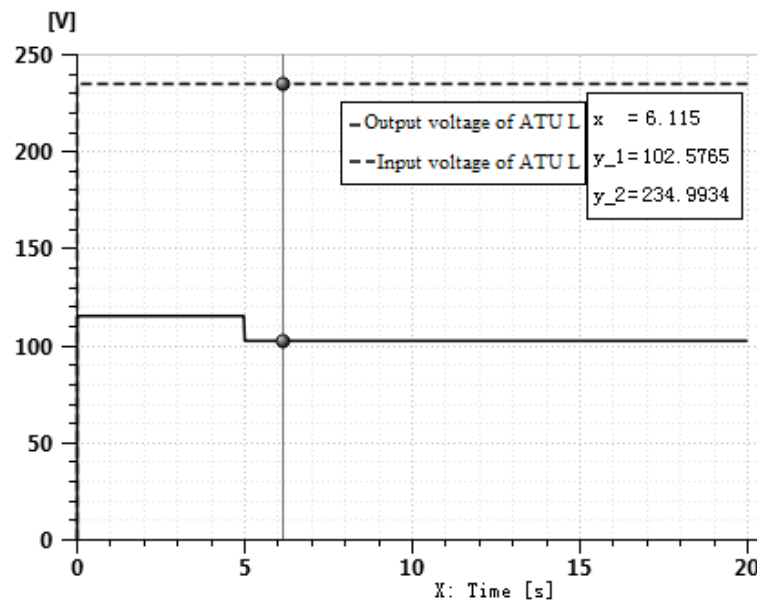


Fig 22: under-voltage of ATU L

(3) Simulation of fault in the bus bar

Fig. 23 illustrates the voltage of loads connected to the 28V bus bar. It can be seen that the voltage of the loads connected to the ports 1~3 drop to 0V at 5s, 7s, and 9s, respectively, which means open circuit fault.

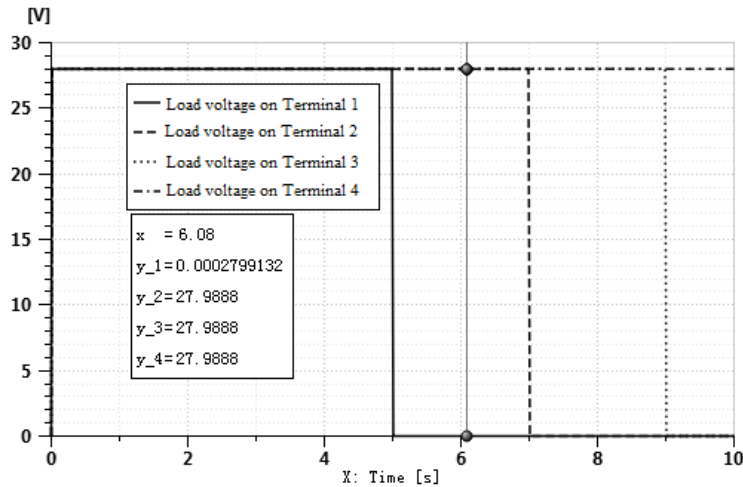


Fig 23: voltage of loads connected to the 28V bus bar

(4) Simulation of fault in the load

Fig. 24 shows the result occurring short circuit fault of load. From this figure, it can be seen that the voltage of the load is small, only 0.028V, when the load occurs short circuit fault. However, a large short-circuit current occurred in the circuit, and the short-circuit current reached 27956.47A. Furthermore, the TRU in the upper level also showed 27956.48A current. The phenomenon is consistent with practical system analysis.

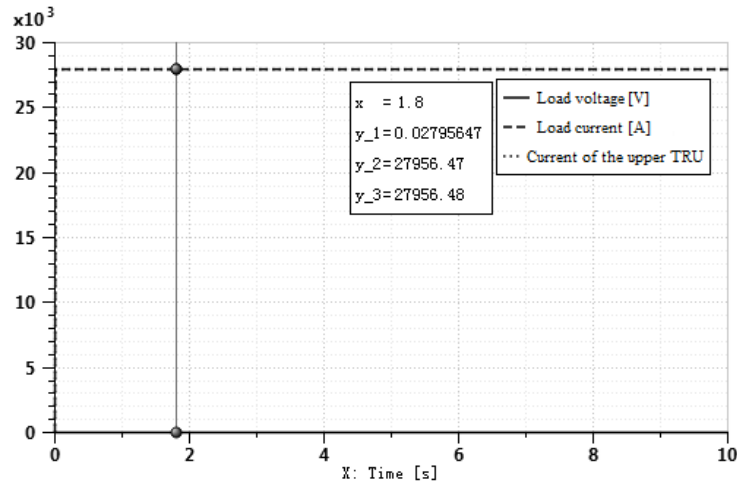


Fig 24: short-circuit fault of load

Fig. 25 provides the result when the power of the load connected to the 28V bus bar which is powered by L_TRU varies. The load power is increased from 280W to 3000W, and then reduced to 1000W. When the load power increases from 280W to 3000W, the input voltage of the load decreases from 28.99V to 28.77V, and the voltage of the bus bar decreases from 28.99V to 28.97V. When the load power decreases from 3000W to 1000W, the voltage of the load increases correspondingly. The fault phenomenon is consistent with practical system analysis.

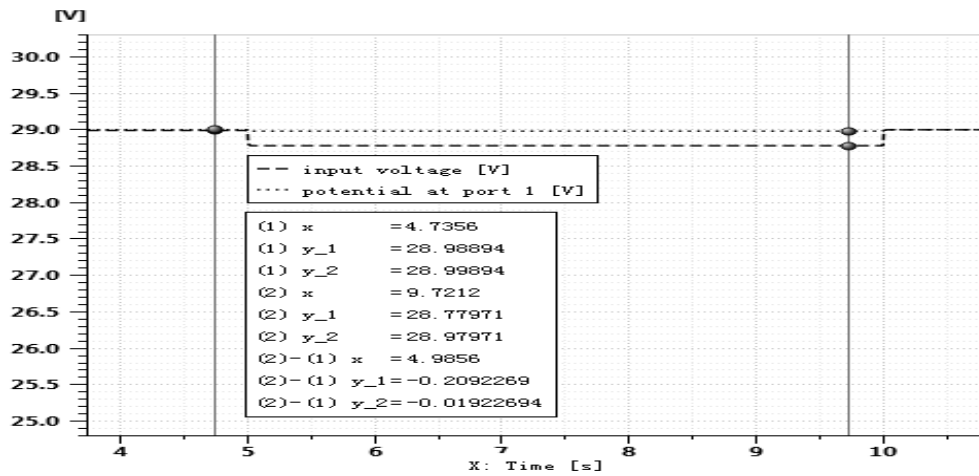


Fig 25: result when the load power varies

(5) Results in the co-simulation platform

Figs. 26~29 illustrate the voltage of the monitoring points 1, 5~7 in the co-simulation platform, when the under-voltage fault occurs to VFSG L1. The voltage of VFSG L1 decreases from 235V to 195V. From these figures, it can be seen that the voltage of the monitoring points also changes correspondingly, which is in line with practical system.

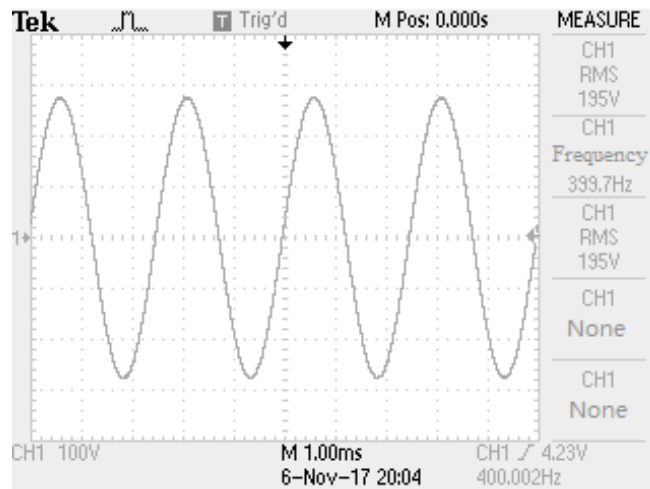


Fig 26: voltage on monitoring point 1

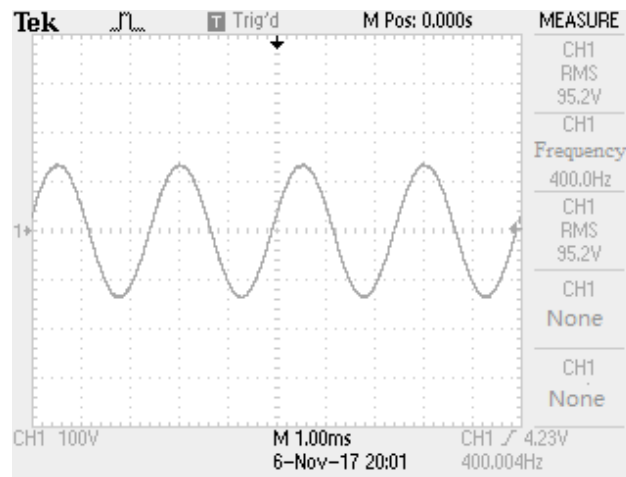


Fig 27: voltage on monitoring point 5



Fig 28: voltage on monitoring point 6



Fig 29: voltage on monitoring point 7

V. CONCLUSION

In this paper, a fault injection model for the electrical system of more electric aircraft has been established for further related research. The mechanism of the electrical system of MEA has been analyzed to reveal its operation principle. Based on these mechanism, the normal model is firstly built in AMESim. Then, fault injection function is added in the normal model to realize fault simulation of the electrical system. Finally, simulation results in the co-simulation platform demonstrated that the fault injection model is able to simulate normal and faulty state of the electrical system in MEA.

The established fault injection model of the electrical system in MEA can also be extended to further related research, such as fault diagnosis, isolation, test, reliability analysis, and so on. Furthermore, the built model can be extended by considering more factors.

ACKNOWLEDGEMENT

This work is supported by National Science Foundation for Young Scientists of China (Grant No. 61703406), and the Natural Science Foundation of Tianjin (18JCQNJC05000).

REFERENCES

- [1] Bourdon J, Asfaux P, Etayo AM (2015) Review of power electronics opportunities to integrate in the more electrical aircraft. International Conference on Electrical Systems for Aircraft
- [2] Zhang Y, Rong S, Wen C, Meng YL, & Gajanayake C (2016) Distributed power allocation and scheduling for electrical power system in more electric aircraft. Conference of the IEEE Industrial Electronics Society
- [3] Guenter S, Buticchi G, Carne GD, Gu C, Liserre M, & He Z (2018) Load Control for the DC Electrical Power Distribution System of the More Electric Aircraft. IEEE Transactions on Power Electronics (99): 1-1
- [4] Madonna V, Giangrande P, Galea M (2018) Electrical Power Generation in Aircraft: review, challenges and opportunities. IEEE Transactions on Transportation Electrification (99): 1-1

- [5] Yicheng Zhang, Rong Su, Changyun Wen, Meng Yeong Lee, Chandana Gajanayake (2016) Distributed power allocation and scheduling for electrical power system in more electric aircraft, Industrial Electronics Society IECON 2016 - 42nd Annual Conference of the IEEE, pp. 102-107
- [6] Chung SS (2012) Method and Apparatus for Fault Injection
- [7] Purvis A, Morris B, Mcwilliam R (2015) Flight Gear as a Tool for Real Time Fault-injection, Detection and Self-repair. Procedia Cirp 38: 283-288
- [8] Foutris, Nikos, Kaliorakis (2014) Versatile architecture-level fault injection framework for reliability evaluation, Proceedings of the 2014 IEEE 20th International On-Line Testing Symposium, pp. 140-145
- [9] Kouwe EVD, Giuffrida C, Tanenbaum AS (2016) Finding fault with fault injection: an empirical exploration of distortion in fault injection experiments. Software Quality Journal, 24(1): 7-36
- [10] Wang Chao, Cui Gang (2011) FSFI: A full system simulator-based fault injection tool. IEEE International Conference on Instrumentation, Measurement, Computer, Communication and Control, pp. 326-329
- [11] Aguirre MA, Tombs JN (2009) Fault injection analysis of bidirectional signals. IEEE Transactions on Nuclear Science 56(4): 2179-2183
- [12] Chang Qing, Chen Jianhui (2007) Design of equipment fault injection system based on BIT, International Conference on Electronic Measurement and Instruments, pp 3362-3365
- [13] Prodan, Lucian (2007) Simulated fault injection for quantum circuits based on simulator commands, International Symposium on Applied Computational Intelligence and Informatics - Proceedings, pp. 245-250, SACI 2007
- [14] 787 Electrical Power System Overview and Component Description 2010-12-02
- [15] Zhen Zhao, Fu-li Wang, Ming-xing Jia, Shu Wang (2011) Modeling and Fault Simulating of Hydraulic Pump on Hydraulic Tube Tester, J, Journal of System Simulation 23(4): 803-807